JOURNAL OF CATALYSIS 102, 64–79 (1986)

Fourier Transform Infrared Study of Butene Adsorption and Reaction on a Silica-Supported Nickel Catalyst

TROY J. CAMPIONE[1] AND JOHN G. EKERDT[2]

Department of Chemical Engineering, The University of Texas at Austin, Austin, Texas 78712

Received December 23, 1985; revised June 10, 1986

The adsorption of 1-butene, *trans*-2-butene, *cis*-2-butene, and 1,1-d_2-1-butene on a well-characterized silica-supported nickel catalyst was studied using Fourier transform infrared spectroscopy. The resultant hydrocarbon surface species were subjected to vacuum and hydrogen. Reaction products were monitored at temperatures from 28 to 100°C. The initial adsorption of each of the *n*-butenes resulted in similar infrared spectra. The main spectral features are proposed to be associated with two surface species: a weakly adsorbed 2,3-dimetallabutane and a strongly adsorbed 1,1,2- and/or 1,1,3-trimetallabutane. The surface orientations of the initially adsorbed metallabutanes are discussed along with the effect of the surface selection rule on the observed infrared bands. Heating the catalyst under vacuum resulted in the desorption of the 2,3-species to form butane and the further dehydrogenation of other metallabutanes. The addition of hydrogen to the initially adsorbed surface species resulted in the evolution of butane and the partial hydrogenation of the strongly adsorbed metallabutanes. The resultant structures were relatively stable in hydrogen at temperatures to 120°C. Evidence was also found for the presence of allylic species during the linear isomerization of the *n*-butenes. It is proposed that allylic species may be precursors to the formation of the metallabutanes as well as possible intermediates in the isomerization reaction.

I. INTRODUCTION

Since the first use of transmission infrared spectroscopy to study the chemisorption and subsequent reactions of molecules on the surface of supported metal catalysts in 1956 (*1*), our understanding of surface–adsorbate interactions has increased substantially. However, in the years following the pioneering infrared studies, little attention has been directed toward the adsorption and reaction of olefins on supported metal catalysts (*2–15*) (much of this work is summarized in Ref. (*16*)).

Morrow and Sheppard (*3*) studied the adsorption of 1-butene on silica-supported Pt and Ni over the temperature range −78 to +95°C. Only absorbances in the C—H stretching region (3200–2800 cm^{-1}) were reported. From these bands, σ-bonded C_4 structures such as those shown in Fig. 1 were proposed as the surface species resulting from the initial adsorption of 1-butene. The relative amounts and the surface orientations of the proposed hydrocarbon surface species were not discussed. Upon hydrogenation of the initially adsorbed species, *n*-butane was observed to evolve from the surface, accompanied by a shift in the location and an increase in the intensity of the initially observed C—H stretching bands. Morrow and Sheppard reported reversible behavior for the infrared bands upon evacuation and readmission of hydrogen. They proposed that an alkyl fragment formed during hydrogenation, in agreement with the earlier findings of Eischens and Pliskin (*2*).

Several investigators reported that the infrared bands resulting from the adsorption of *cis*-2-butene and *trans*-2-butene were essentially the same as for the adsorption of 1-butene (*2, 7, 17*). Adsorption of the isomers of *n*-pentene has also been reported to

[1] Present address: Exxon Chemical Company, P.O. Box 241, Baton Rouge, La. 70821.

[2] To whom correspondence should be addressed.

0021-9517/86 $3.00

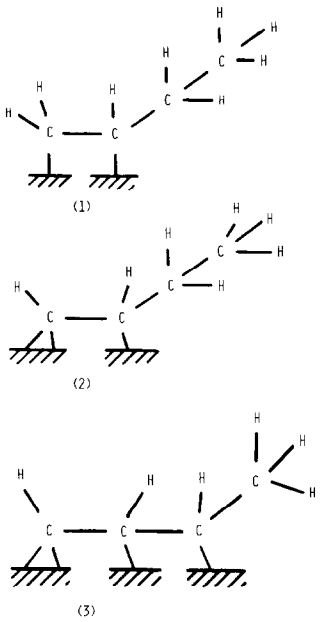

FIG. 1. Proposed hydrocarbon surface species resulting from the adsorption of 1-butene onto Ni/SiO_2 and Pt/SiO_2 catalysts at −70 to 95°C.

result in similar infrared spectra (*2*). From these findings, it was suggested that a common surface species was responsible for the observed absorbances. Multiply bound species, such as those shown in Fig. 1, were proposed as the chemisorbed structures resulting from the initial adsorption of the isomers of *n*-butene.

The interpretation of the infrared spectra of adsorbed chemical species is not straightforward. The existence of multiple surface species, electronic effects induced by the metal (*18*) and the influence of the surface selection rule (*18, 19*) pose significant complications. Greenler *et al.* (*18*) discussed the changes in the infrared absorption intensities for a molecule adsorbed on the surface of a metal sphere that is a good conductor. They examined the ratio, SR, of the infrared absorption intensities for a dipole moment oscillating parallel to the surface to one oscillating perpendicular to the surface. The value of SR is bounded by 2 and 0. SR is 2 when the sphere does not perturb the oscillating dipoles in any way (this value is also calculated for a hemisphere). SR is 0 when the dipole oscillating parallel to the surface is completely cancelled by an image dipole of opposite direction in the metal. Similarly, the image dipole for vibrations oriented perpendicular to the surface acts to increase the absorbance intensity for the perpendicular vibration (*19*). This cancellation and enhancement phenomena is referred to as the surface selection rule.

The observed ratio of intensities from vibrations parallel and perpendicular to the surface should be given by the ratio of their intensities in the absence of surface effects multiplied by SR (*18*). The value of SR was found to be insensitive to metal type and infrared region, but is a strong function of sphere size (increasing as the radius decreases) and the distance of the vibration away from the sphere's surface (increasing as the distance increases). (In the present study a terminal methyl group of an adsorbed *n*-butyl, with a C—Ni bond distance of 2 Å, would be at most 5.77 Å from the surface. The value of SR associated with the vibrations this distance from the surface of a 108 Å diameter sphere is estimated to be 0.023. Therefore, the parallel components of any vibrations for C_4 structures will be subject to attenuation, by the surface selection rule.)

The effects of the surface selection rule are observed and recognized for work on single crystal substrates (*20*). However, few infrared studies on supported-metal catalysts, where the metal particles are dispersed on a nonconducting support such as SiO_2, have dealt with this possible influence (*14, 19*). This point is significant since much of the interpretation of infrared spectra for adsorbed hydrocarbons in the past was based on the relative intensities of bands observed in the C—H stretching region. The attenuation and/or enhancement of the intensity of any of the bands could significantly alter the conclusions of these earlier studies.

The presence of π-bonded olefins and/or

allylic species should be anticipated in addition to the more stable surface species that remain on a catalyst surface following the adsorption and reaction of an olefin. Allylic species have been proposed as the intermediates in the isomerization of olefins over metals (*21, 22*) and metal oxides (*23–26*). Prentice *et al.* (*27*) reported infrared evidence for the π-bonding of ethylene on silica-supported Pt and Pd. The literature is void of infrared evidence for the π-allyl complexes on silica-supported metal catalysts.

The purpose of this study was to identify and characterize the surface species formed when each of the *n*-butenes was adsorbed and reacted on a Ni/SiO_2 catalyst.

II. METHODS

A. Apparatus

All of the infrared spectra were recorded on a Digilab FTS-15/90 FTIR at a resolution of 2 cm^{-1}. A MCT detector was used to maximize the detectivity of the spectrometer over the spectral range of 3300–500 cm^{-1}. This feature was important since infrared absorbances for the adsorbed hydrocarbon species were typically very weak (0.005–0.05 absolute absorbance units) compared to those for the background absorbance of the catalyst disk (0.1–0.4 absolute absorbance units at 3200 cm^{-1}).

The infrared cell was fabricated by modifying a standard 2-3/4-in. o.d. Huntington stainless-steel butterfly valve (Fig. 2). A removable catalyst disk holder was attached to the stem so that it was possible to rotate the disk into or out of the infrared beam. This enabled the collection of gas phase spectra when desired. The incorporation of three 150-W high intensity cartridge heaters enabled temperatures of up to 425°C to be attained. Modifications were made to water-cool the Viton O-ring valve stem seals. A stainless-steel sheathed thermocouple was positioned approximately 1 mm from the center of the mounted catalyst disk. Cell pressures from 1 mTorr to 1 atm were measured using a Varian thermocouple vacuum gauge and a Validyne DP-15 pressure transducer. O-Ring mounted KBr optics (Janos Optical) were used.

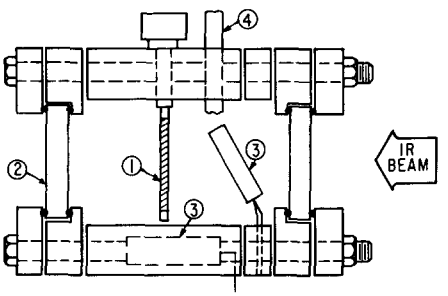

FIG. 2. Infrared cell design. (1) Catalyst disk mounted on rotatable valve stem; (2) O-ring mounted KBr optics; (3) cartridge heaters; (4) feedthroughs for pressure transducer, thermocouple, vacuum valves, radiant heater, and cooling water.

A schematic of the infrared reactor system is shown in Fig. 3. A stainless-steel Ultra-Torr tee, fitted with a septum, was used to sample the gas phase and admit hydrocarbons into the infrared cell. This technique ensured uncontaminated sample transfer and minimized the waste of labeled compounds. Gas samples were analyzed for C_1 to C_6 hydrocarbons using a Hewlett–Packard 5880 gas chromotograph.

The temperature-programmed desorption apparatus was typical of those used for powdered catalyst studies. The chemisorption manifold consisted of a conventional glass vacuum system and precise pressure measuring devices and has been described in an earlier study (*28*). Additional details of the analytical equipment and systems used in this study may be found in Ref. (*29*).

B. Procedure

Catalyst preparation and characterization. An 8.29 wt% silica-supported nickel catalyst was prepared using the wet-impregnation technique. Nickel nitrate hexahydrate was dissolved in ultrapurified water (18 Mohm-cm resistivity). This solution was then slowly added, with constant stir-

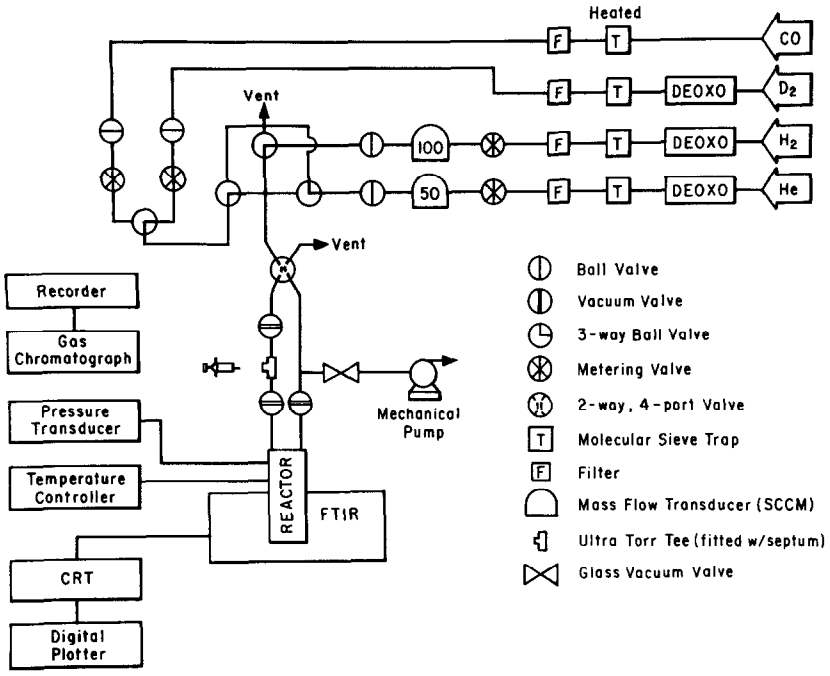

FIG. 3. Infrared system schematic.

ring, to dry silica (Cab-O-Sil HS-5, Cabot Corp., 325 m^2/g). The resultant paste was slowly dried (approximately 1 hr) at 50–120°C on a hot plate with constant stirring. The powdery catalyst was then crushed and sieved to 325 mesh. The entire batch of catalyst was then loaded into a quartz tube fitted with a quartz frit, and placed in an oven. The catalyst was pretreated in argon, reduced in hydrogen and passivated in air. The catalyst preparation schedule is given in Table 1. (A more complete discussion of catalyst preparation is given in Ref. (*29*).) After the catalyst was cooled in hydrogen to 30°C at the end of the reduction period, it was allowed to come slowly in contact with air.

TABLE 1

Catalyst Preparation Schedule

	Temperature (°C)	Ramp rate (°C/min)
	25–90	2
	90–120	1
Degas	120–200	2
(50 cm^3/min Ar)	200–250	1
	250–400	3
	400	(2 hr hold)
	30–200	2
Reduction	200–250	1
(50 cm^3/min H_2)	250–375	3
	375	(4 hr hold)

Transmission electron microscopy measurements were conducted using a Siemens Elmiskop I electron microscope, capable of better than 3 Å resolution. The catalyst sample was examined at a magnification of 48,000×. Approximately 450 particles were counted from enlarged photographs at a magnification of 226,000×. It was possible to distinguish metal crystallites of approximately 10 Å diameter and larger from the silica support.

Hydrogen uptake studies were performed at 25°C. A bare nickel surface was prepared by evacuating the freshly reduced catalyst at 360°C for 30 min to a pressure less than 1 mTorr. Twenty minutes were

TABLE 2

Ni/SiO_2 Catalyst Characterization

wt% Ni[a]	H_2 Uptake[b]	O_2 Uptake[c]	% Reduction[d]	% Dispersion[e]	Avg. particle size (Å)	
					d_{sH_2}[f]	d_{sTEM}[g]
8.29	61.0	677.0	96.0	9.0	108	147

[a] Analysis by Galbraith Laboratories, Inc.
[b] μmoles/g catalyst H_2 adsorbed at monolayer coverage at 27°C.
[c] μmoles/g catalyst O_2 reacted with the reduced nickel catalyst at 375°C.
[d] Percentage reduction of nickel catalyst to the metal based on O_2 titration at 375°C.
[e] Percentage of nickel surface available for chemisorption.
[f] Surface-averaged nickel crystallite diameter from H_2 uptake data.
[g] Surface-averaged nickel crystallite diameter calculated using electron microscope results.

allowed for equilibration between each pressure measurement. The Langmuir model for dissociative adsorption was used to determine the number of moles of H_2 adsorbed at monolayer coverage. A ratio of one hydrogen atom to one surface Ni atom was used to estimate metal particle size.

The extent of reduction to metallic nickel was measured for the Ni/SiO_2 catalyst by oxygen titration. The catalyst was reduced as in the hydrogen uptake studies. Total oxygen uptake was measured at 375°C following a 4-hr evacuation at that temperature to a pressure of less than 0.1 mTorr. The results of the catalyst characterization studies are reported in Table 2.

Infrared studies. Approximately 100–200 mg of prereduced catalyst powder was pressed into a 0.1–0.2-mm-thick wafer using a 1-in.-diameter stainless-steel die and 3000–5000 lb force over a period of 2–4 min. The disk was then loaded into the infrared cell and degassed under vacuum as the temperature was raised (approximately 5°C/min) to 140°C. After holding this temperature for 30 min, the disk was cooled to 50°C or below and hydrogen was slowly admitted to a pressure of 1 atm. A steady state flow rate of 50 cm^3/min H_2 was established, then the disk was ramped (5°C/min) to 360° where it was maintained for 2 hr. After the reduction period, the cell was allowed to cool to 28°C in flowing H_2. An evacuation period of 1–15 min was implemented to remove hydrogen selectively from the catalyst surface. Catalyst disks prepared in this manner were referred to as "hydrogen-covered." The resultant degree of hydrogen coverage is discussed later. A fresh catalyst disk was used for each experiment to eliminate complicating factors such as the deposition of carbidic species on the nickel surface sites.

Reference spectra of the empty chamber and of the catalyst disk were taken prior to the addition of the olefin. Hydrocarbons were injected into the evacuated cell using a gas-tight syringe. Syringes were thoroughly cleaned before sample handling. The purity of each injection was ascertained by injecting the residual gas into the gas chromatograph.

After a dosing period of 15 min, the gas phase was sampled via syringe and analyzed using gas chromatography. The cell was then briefly evacuated (approximately 1 min) to a pressure of approximately 5 mTorr to remove reaction products and any physically adsorbed molecules. Fifty to one hundred scans were required to obtain quality spectra of the hydrocarbon surface species.

The effect of adding hydrogen to the surface species was studied by admitting con-

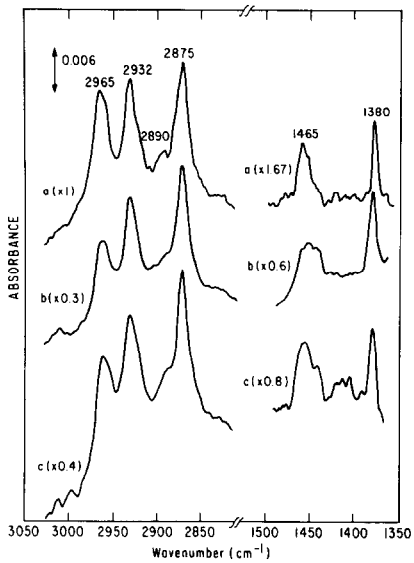

FIG. 4. *n*-Butene adsorption on a hydrogen-covered surface at 28°C. (a) 1-Butene dosed at 49 Torr, (b) *cis*-2-butene dosed at 40 Torr, (c) *trans*-2-butene dosed at 20 Torr.

trolled amounts of hydrogen into the cell and observing changes in the spectra and gas phase composition.

Temperature-programmed desorption studies. Approximately 40 mg of prereduced catalyst was loaded into the quartz tube reactor, degassed in 50 cm^3/min He for 30 min at 140°C, then reduced in 50 cm^3/min H_2 for 2 hr at 360°C. Heating rates comparable to those used in the infrared studies were used to attain the final temperature. After the reduction period, the reactor was cooled in flowing H_2. Helium (50 cm^3/min) was then flowed through the catalyst bed for 7 min to simulate the brief evacuation period employed in the infrared studies. Next, the reactor was isolated while a 47.3 cm^3/min He : 2.7 cm^3/min 1-butene stream was established and stabilized. This mixture approximated the typical butene partial pressure used in a dose for the infrared experiments. The catalyst was exposed to this stream for 1 min and then isolated. After a "dosing period" of 15 min, He at 50 cm^3/min flowed through the catalyst bed. The reactor effluent was monitored using mass spectroscopy. Samples of the reactor effluent were stored in the loops of a multiport sampling valve at regular intervals for later analysis by gas chromatography.

C. Materials

Hydrogen (99.999%), argon (99.999%), and helium (99.995%) were purified further with oxygen scrubbers (Chromopon or Matheson) and sodium alumino silicate 13 X molecular sieve traps (Matheson or in-house). Hydrocarbon gases: 1-butene (99.9%, Matheson), *cis*-2-butene (96.0%, Union Carbide), *trans*-2-butene (99.4%, Union Carbide), and 1,1-d_2-1-butene (98.6% MSD Isotopes) were used without further purification. Oxygen (99.995%, Big Three) was passed through a molecular sieve trap before use.

Nickel nitrate hexahydrate (Aldrich Chemical Co.) was analyzed to be 19.6 wt% Ni with trace impurities of Mg, Si, Fe, and Cu at concentrations of 0.5–2.0 ppm.

III. RESULTS

A. Adsorption of the n-Butenes at 28°C

The adsorption of 1-butene, *cis*-2-butene, and *trans*-2-butene onto a hydrogen-covered catalyst surface at 28°C resulted in similar spectra as seen in Fig. 4. The hydrocarbon surface species were characterized by three major peaks in the C—H stretching region at 2965, 2932, and 2875 cm^{-1}, and two major peaks in the C—H deformation region at 1465 and 1380 cm^{-1}. An additional peak of lesser intensity was also observed in the C—H stretching region at approximately 2890 cm^{-1}. It is proposed that these absorbances correspond to the presence of two dominant sp^3-hybridized surface species: a weakly adsorbed 2,3-dimetallabutane and a strongly adsorbed 1,1,3- and/or 1,1,2-trimetallabutane. Only *n*-butane and the linear butene isomers were detected in the gas phase after the 15-min dosing periods of each of the *n*-butenes.

The term "hydrogen-covered" was introduced in an earlier infrared study (*2*) and

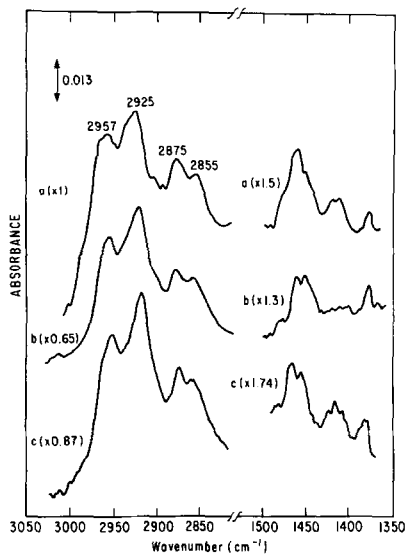

FIG. 5. Hydrogenation of the initially adsorbed *n*-butenes at 28°C. (a) 1-Butene, (b) *cis*-2-butene, (c) *trans*-2-butene.

refers to partial hydrogen coverage of the catalyst surface, resulting from the 1- to 15-min evacuation period, prior to the admission of the olefin. Approximately 20% of a monolayer of hydrogen was pumped off the catalyst surface in 3 min while 50% was removed in 15 min at 28°C. These values were obtained by performing hydrogen uptake studies at 28°C on the bare catalyst surface and on surfaces that were saturated with hydrogen at 760 Torr and subsequently evacuated for 3 and 15 min. The evacuation period prior to dosing the olefin was typically 3 min and never exceeded 15 min. Therefore, at least half of the surface sites capable of adsorbing hydrogen were covered prior to the admission of the butenes into the cell.

B. Hydrogenation of the Initially Adsorbed Species

Figure 5 shows the result of reacting the surface species, resulting from the initial adsorption of the *n*-butenes, with hydrogen at 28°C. *n*-Butane was the only reaction product detected upon the addition of hydrogen to the cell. The spectral changes resulting from the hydrogenation reaction were characterized by: shifts in position of the 2965- and 2932-cm^{-1} bands to 2957 and 2925 cm^{-1}, respectively, in conjunction with a change in their relative intensity; a decrease of more than half of the original intensity of the 2875-cm^{-1} band; the emergence of a new band at 2855 cm^{-1}, corresponding to $\nu_{sy}CH_2$; and, a change in the relative intensity of the $\delta_{as}CH_3$ and $\delta_{sy}CH_3$ bands at 1465 and 1380 cm^{-1}, respectively. The broad absorbance at 1415 cm^{-1} was found to increase slightly in intensity upon the addition of hydrogen to the catalyst.

When a vacuum was applied to the cell after hydrogen treatment of the initially adsorbed species, all of the bands decreased slightly in intensity, suggesting the removal of hydrocarbons from the surface to the gas phase and/or the dehydrogenation of the surface species. Depending on the conditions of the initial adsorption of the *n*-butene onto the catalyst surface, the readmission of hydrogen sometimes resulted in a reversible effect where much of the original band intensities were restored. Rehydrogenation was not studied.

C. Heating Adsorbed Species under Vacuum

Figure 6 displays the infrared spectra for the initial adsorption of 1-butene onto a hydrogen-covered surface and for the subsequent heating of the adsorbed species to 40 and 48°C under vacuum. Upon heating, the absorbances at 2875 and 1380 cm^{-1} lost more than 60% of their original intensities, while the bands at 2965, 2932, and 1465 cm^{-1} were only mildly attenuated. The majority of the intensity attenuation of the 2875- and 1380-cm^{-1} bands occurred at approximately 40°C. (Infrared spectra were recorded at 3°C intervals as the catalyst temperature was raised to 80°C.) No significant changes in the intensities of any of the bands were apparent in the temperature range 50–80°C.

The intensity of a band at 1415 cm^{-1} grew steadily as the catalyst was heated to 70°C,

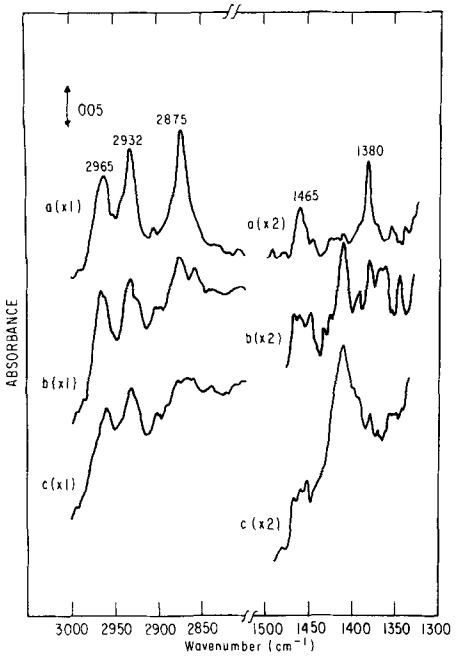

FIG. 6. 1-Butene adsorption at 28°C and subsequent heating under vacuum (dosing pressure = 40 Torr). (a) Adsorption on a hydrogen-covered surface; (b) heated under vacuum to 40°C; (c) heated under vacuum to 48°C.

at which point it leveled off. The intensity increase of this band with temperature was correlated to the formation of a severely dehydrogenated surface species.

The gas phase was monitored by gas chromatography as the cell was heated. Only *n*-butane and the isomers of *n*-butene were detected. No cracking of the C_4 hydrocarbon structure was observed below 80°C. Above this temperature butane and propane were detected in the gas phase.

D. Adsorption of 1,1-d_2-1-Butene at 28°C

The spectrum resulting from a 50-Torr dose of 1,1-d_2-1-butene onto a hydrogen-covered surface at 28°C is shown in Fig. 7 and is similar to those obtained in the *n*-butene studies, except that the absorbances at 2875 and 1380 cm^{-1} were attenuated by 30–40%, relative to the absorbances at 2932 and 1465 cm^{-1}, respectively. Additional peaks were observed in the C—D stretching region (2200–1900 cm^{-1}) but were weak (<0.002 absorbance units) and did not indicate significant H/D scrambling. Bands at 1415 cm^{-1} and a shoulder at 1483 cm^{-1} appeared in the deformation region of the spectrum and were assigned to CH_x deformations of the surface species. An analysis of the gas phase reaction products, after the 15-min dose, was similar to that for the reaction of 1-butene. When the surface species generated by the adsorption of 1,1-d_2-1-butene onto a hydrogen-covered surface were exposed to 300 Torr of hydrogen at 28°C, the result, shown in Fig. 7 was similar to that obtained in the *n*-butene hydrogenation studies. The above findings indicate that the reactivity of the deuterim-substituted butene is very similar to that of 1-butene.

E. Temperature-Programmed Desorption Studies

A temperature-programmed desorption study was conducted to determine whether the major spectral changes depicted in Fig. 6, for heating the surface species under vacuum, were associated with the desorption of a hydrocarbon species. 1-Butene, at a partial pressure of 40 Torr in helium, was adsorbed onto the hydrogen-covered cata-

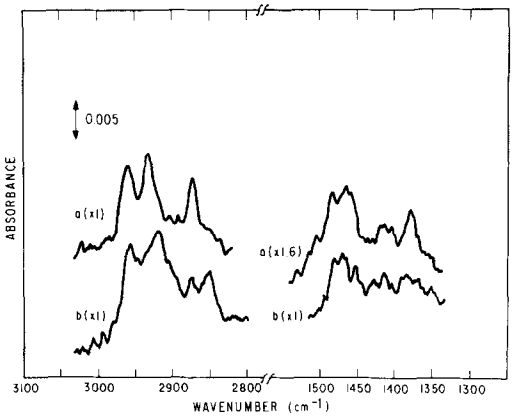

FIG. 7. 1,1-d_2-1-Butene adsorption and hydrogenation at 28°C (dosing pressure = 50 Torr). (a) Adsorption on hydrogen-covered surface; (b) following 300 Torr H_2.

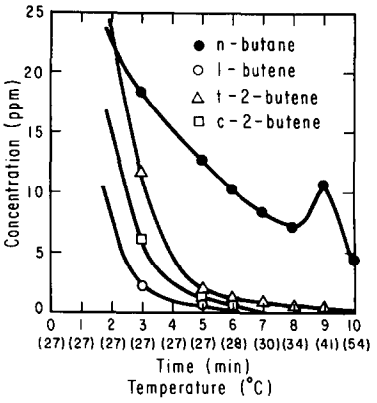

FIG. 8. Temperature-programmed desorption results for the 1-butene dosed catalyst.

lyst at 28°C. (See Methods for a complete listing of the procedure.) The reactor effluent was sampled periodically and analyzed by gas chromatography. The composition of the reactor effluent is shown in Fig. 8 as a function of catalyst temperature. The desorption maximum at approximately 40°C for the *n*-butane was correlated with the observed losses in intensity of the bands at 2875 and 1380 cm^{-1} shown in Fig. 6.

III. DISCUSSION

The interpretation of the spectra resulting from the initial adsorption of the *n*-butenes was aided by the fact that the C_4 skeleton of the reacted hydrocarbons remained intact at temperatures ranging from 28 to 80°C. Analysis of the gas phase above the catalyst disk, in this temperature regime, revealed only *n*-butane and the isomers of *n*-butene. Therefore, only surface structures involving a chain of four carbon atoms were considered in the interpretation of the spectra. Figure 9 summarizes the species proposed to form and their reaction products.

A. Evidence for the 2,3-Dimetallabutane

The spectrum shown in Fig. 10 is representative of the results for the initial adsorption of each of the *n*-butenes onto a

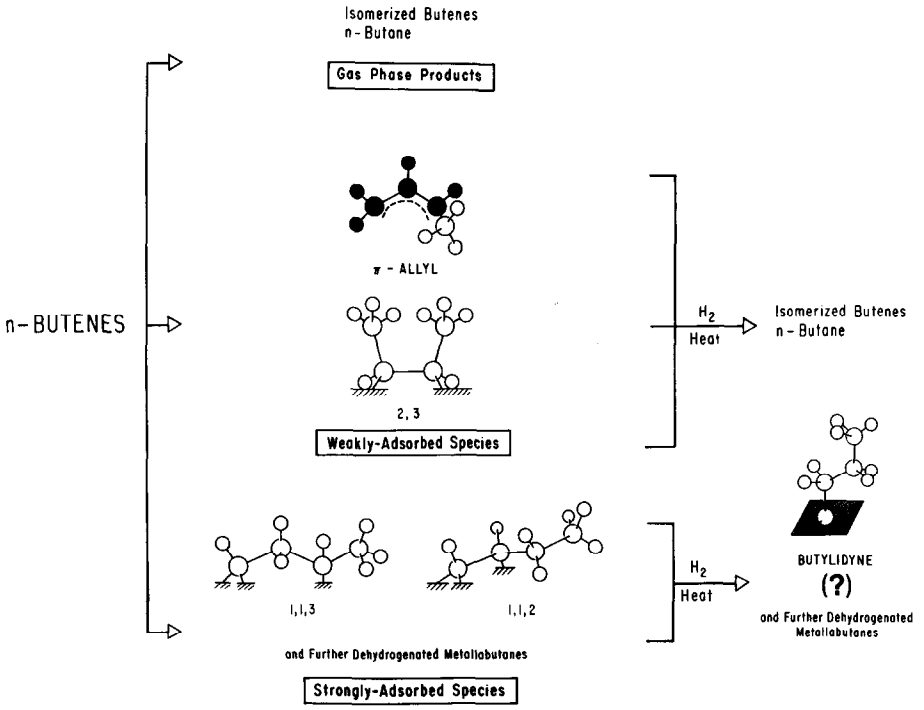

FIG. 9. Overall scheme for the adsorption and reaction of the linear butenes.

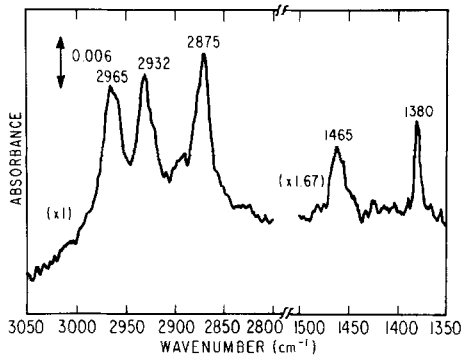

FIG. 10. 1-Butene adsorption onto a hydrogen-covered surface at 28°C (dosing pressure = 49 Torr).

hydrogen-covered surface. An analysis of this spectrum resulted in two important observations: first, the intensity of the 2875-cm^{-1} absorbance, a band normally assigned to $\nu_{sy}CH_3$, was the largest in the spectrum and second, the intensity of the band at 1380 cm^{-1}, representing the $\delta_{sy}CH_3$ vibration, was much greater than expected from a comparison to the intensity of the absorbance at 1465 cm^{-1}, corresponding to the overlap of $\delta_{as}CH_3$ and $\delta_{sy}CH_2$ (see Refs. (*30, 31*) for infrared frequency assignments for hydrocarbon molecules.)

The relative absorbance intensity values for typical hydrocarbon groupings, as well as frequency assignments for the various CH_x groups found in alkanes, are presented in Table 3. These values indicate that, for a typical methyl group in a straight chain alkane in solution, the absolute intensity of the 1380-cm^{-1} absorbance is nearly equal to that of the 1465-cm^{-1} absorbance. Table 4 provides a list of band intensities (absorbance at peak maximum) and assignments for the infrared bands resulting from the adsorption of 1-butene onto a hydrogen-covered surface (Fig. 10). Table 5 lists the relative band intensities of several bands of interest in Fig. 10 and compares these relative values to those expected for normal alkanes in solution. (Absolute intensities are presented in Table 4 rather than integrated intensities. The overlap of bands, particularly in the C—H stretching region, prevented their accurate deconvolution. While the integrated band area would be more precise, the use of absolute absorbance is appropriate here because the absolute absorbance is related to species concentration and because the absolute intensities could be compared to published values for intensities at peak maximum (*31, 32*).)

TABLE 3

Frequency Assignments and Absolute Intensities for Hydrocarbon Groupings

Group	Vibration (*30*)	Frequency (cm^{-1}) (*30, 31*)	Absolute Intensity per group (ε_{max}) (*31, 32*)
CH_3	ν_{as}	2955 ± 5	129
	ν_{sy}	2870 ± 5	55
	δ_{as}	1462 ± 5	17.5
	δ_{sy}	1380	20.5
CH_2	ν_{as}	2927 ± 5	77
	ν_{sy}	2855 ± 5	46
	δ_{sy}	1467	8
CH	ν	2890	—

The I_{2965}/I_{1380} and I_{1465}/I_{1380} intensity ratios were significantly different from what were expected for alkanes. The electronic effects of the metal on the absorbance ratios cannot be predicted precisely; however, asymmetric CH_3 modes (2965 and 1465 cm^{-1}) for the 2,3-dimetallabutane

TABLE 4

Frequency Assignments and Absolute Intensities for the Absorbances in Fig. 10

cm^{-1}	Absolute absorbance ($\times 6 \times 10^{+4}$)	Assignment
2965	22	$\nu_{as}CH_3$
2932	21	$\nu_{as}CH_2$
2890	5	νCH
2875	25	$\nu_{sy}CH_3$
1465	7	$\delta_{as}CH_3 + \delta_{sy}CH_2$
1380	10	$\delta_{sy}CH_3$

TABLE 5

Relative Absorbance Intensities Compared to Expected Values for the Absorbances in Fig. 10

	Observed	Expected[a]
$\frac{I_{2965}}{I_{2875}} =$	0.88	2.3
$\frac{I_{2965}}{I_{1380}} =$	2.2	6.3
$\frac{I_{1465}}{I_{1380}} =$	0.7	$\geq 1.2^b$

[a] On the basis of the *n*-alkane data in Table 3.

[b] Calculated assuming one or more CH_2 groups present for each CH_3 group.

structure proposed below are primarily parallel to the surface and this should act (in the limit that SR equals 2) to increase the expected values listed in Table 5, assuming the Ni particles are hemispherical in shape.

The observed ratios suggest that there was intensity enhancement of the symmetric CH_3 vibrations (2875 and 1380 cm^{-1}) relative to the asymmetric CH_3 vibrations (2965 and 1465 cm^{-1}) of the hydrocarbon surface species. Supporting evidence is provided by the I_{2965}/I_{2875} ratio, that is significantly different from what would be expected. (Contributions to the intensity of the 2875 cm^{-1} absorbance by the $\nu_{sy}CH_2$ mode were not expected for reasons discussed later.)

Significant changes in the intensities of the bands at 2875 and 1380 cm^{-1} occurred upon heating the surface species, generated by the adsorption of 1-butene onto a hydrogen-covered surface, in vacuum. Sharp decreases in the intensities of these bands occurred at approximately 40°C. A gradual decrease in the intensities of the bands at 2965 and 2932 cm^{-1} was also observed as the catalyst was heated to 80°C. The attenuation of the 2875- and 1380-cm^{-1} absorbances was attributed to the desorption of a weakly adsorbed species from the catalyst surface, while the losses in the 2965- and 2932-cm^{-1} absorbances were related to the dehydrogenation of a more strongly adsorbed species.

During a temperature-programmed desorption study (Fig. 8) the concentration of each of the olefins displayed a continuous decay with increasing temperature. This phenomenon was probably associated with a chromatographic effect as the gases passed through the quartz reactor and sections of unheated gas transfer lines. The desorption of hydrocarbons from the surface of the nickel catalyst was also possible. Butane displayed a peak at 40°C. A weakly adsorbed 2,3-dimetallabutane (Fig. 11) is proposed as the species responsible for the majority of the intensity of the bands at 2875 and 1380 cm^{-1} that were attenuated near 40°C and the *n*-butane desorption peak shown in Fig. 8 at 40°C. (The hydrogen needed to form *n*-butane presumably came from other coadsorbed hydrocarbon species.) The weakly held species is proposed to be as saturated as possible with hydrogen since butane rather than butene formed upon desorption.

The orientation shown in Fig. 11 for the 2,3-species has the 1–2 and 3–4 C—C bond axes of the C_4 structure nearly perpendicular to the surface. This structure was arrived at by using molecular models in which the bond angles were restricted to those for sp^3-hybridized molecules and can be accommodated on the various low energy close-packed nickel planes, Ni(111) and

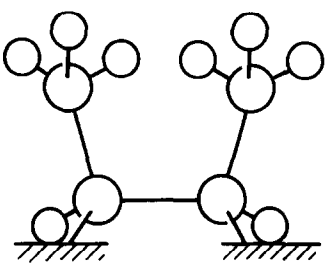

2,3

FIG. 11. Adsorbed orientation and structure for the 2,3-dimetallabutane species.

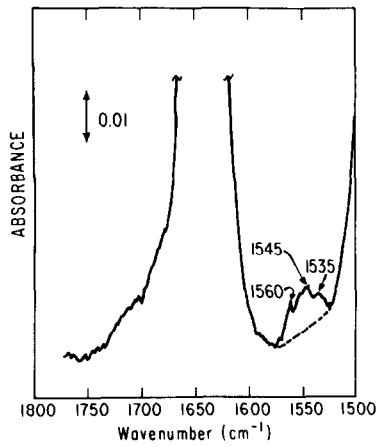

FIG. 12. Evidence for allylic species during the isomerization of 1-butene (dosing pressure = 49 Torr).

Ni(100), by bonding the 2 and 3 carbons to different surface nickel atoms and using reported Ni lattice spacings (*33*). The methyl groups are estimated to be 3.26 Å away from the surface. For a 108-Å Ni particle, the formula developed by Greenler *et al.* (*18*) predicts a ratio, SR, of 0.0073 for the parallel to the perpendicular components of the methyl vibrational modes.

The dipole moments for the asymmetric methyl stretch (2965 cm^{-1}) and asymmetric methyl deformation (1465 cm^{-1}) are in a plane nearly perpendicular to the 1–2 and 3–4 C—C bond axes while the symmetric methyl stretch (2875 cm^{-1}) and asymmetric methyl deformation (1380 cm^{-1}) dipole moments are directed along these C—C axes. The orientation of the 2,3-dimetallabutane (see above) would result in the asymmetric modes vibrating nearly parallel to the surface and the asymmetric modes vibrating nearly perpendicular to the surface. The net effect of the surface selection rule on the absorbances of the proposed, 2,3-species is that the majority of the asymmetric vibrations are attenuated while the symmetric vibrations are enhanced.

Figure 7 shows the attenuation of the bands at 2875 and 1380 cm^{-1} by approximately $\frac{1}{3}$ when 1,1-d_2-1-butene was adsorbed onto a hydrogen-covered surface. As a rough approximation, $\frac{1}{3}$ of the intensity of these bands would be expected to be lost if the majority of their intensity were due to the 2,3-species since two of the six methyl hydrogens would be substituted by deuterium. These results are influenced by H/D exchange. The extent of H/D exchange was not quantified; however, additional studies (*29*) suggest that minimal H/D exchange occurred during adsorption.

B. Evidence for Allylic Species

In an attempt to observe the surface species involved in the linear isomerization of 1-butene, infrared spectra were recorded prior to the evacuation of the gas phase from the cell. It was possible to make a distinction between the absorbance due to gas phase molecules and the surface species in the region 1500–1700 cm^{-1}. The spectrum in Fig. 12 shows a group of bands centered at approximately 1545 cm^{-1} that was assigned to allylic species on the catalyst surface. These bands disappeared upon evacuation of the cell, reflecting the highly unstable nature of these complexes.

π-Bonded and allylic complexes were historically thought to have most of their stretching vibrations in the plane of the coordinated C=C bond. H-NMR studies have shown that there is a negative repulsion of the olefinic hydrogens or other hydrocarbon substituents out of the C—C plane and away from the metal by as much as 8–25 degrees (*34, 35*). Also, as a general rule, the metal atom is closer to the less-substituted carbon atom of the shared bond (*36, 37*). This phenomenon is attributed to both steric and electronic factors. For π-allyl complexes, this results in the tilting of the plane of the three carbon atoms involved in bond sharing with respect to the metal–allyl bond axis, or a plane normal to the metal coordination plane (*38*), i.e., the terminal allylic carbon atoms are further from the metal atom than the central allylic carbon atom. X-Ray studies (*39*) also suggest that the two C⋯C bonds in an allylic complex are not of equal lengths. These

structural orientations suggest that if the plane of the allylic carbons are also tilted relative to the Ni surface plane, it should be possible to observe some of the $\nu C \cdots C$, $\nu C \cdots C \cdots C$, and $\nu C—H$ modes of π and π-allyl complexed olefins on supported metal crystallites, even under the restrictions of the surface selection rule.

The $C \cdots C \cdots C$ stretching frequencies, reported in the organometallic literature for allylic complexes with nickel, are typically 30 to 100 cm^{-1} lower than those reported herein; however, these values (*40, 41*) are for the complexing of propylene. Allylic complexes of C_4 olefins may exhibit a somewhat smaller frequency shift (*42*) relative to the C=C bond of the olefin. For example, allylic complexes of butene with iron and palladium exhibit absorbances at 1510 to 1527 cm^{-1} (*43, 44*). While less than expected from organometallic complexes, the observed shift for $\nu C \cdots C \cdots C$ in this study was reasonable since a weaker metal–hydrocarbon interaction could account for the wavenumber difference (*45*). Similar arguments were advanced for the assignment of allylic species on ZnO (*25, 42*).

The initial adsorption of *n*-butenes resulted in linear isomerization and the appearance of absorbance bands indicative of allylic species. The absorbance bands were only detected in the presence of gas phase *n*-butenes. These observations suggest that allyls may be associated with the isomerization reactions. However, the importance of allylic species in butene isomerization over Ni cannot be established from the infrared results. Furthermore, since the initial adsorption of each of the *n*-butenes resulted in essentially the same spectrum (Fig. 4), it is proposed that a common precursor was responsible for the formation of the surface species. The precursor could be an allyl.

C. Evidence for Trimetallabutanes

Two structures, 1,1,3- and 1,1,2-trimetallabutane (Fig. 13), are proposed to form during adsorption on a hydrogen-covered surface. The bands at 2965, 2932, 2890, and

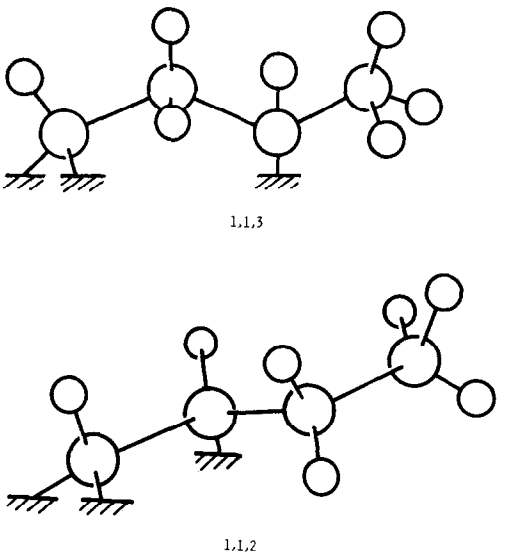

FIG. 13. Adsorbed orientation and structure for the 1,1,3-trimetallabutane and the 1,1,2-trimetallabutane species.

1465 cm^{-1} are thought to be associated with the trimetallabutanes. Contributions to the $\nu_{as}CH_3$ absorbance at 2965 cm^{-1} by the 2,3-dimetallabutane species are expected to be minor due to the effect of the surface selection rule on this 2,3-species' vibrations. The structures presented in Fig. 13 and their respective infrared assignments are consistent with the following observations. (1) The $\nu_{sy}CH_2$ stretching band was not observed upon the initial adsorption of butene. (2) The intensity and location of the $\nu_{as}CH_2$ bands, observed with the hydrogenated and deuterated adsorbates, suggest that only one type of CH_2 group was present and that it was not on a terminal carbon atom. (3) The appearance of a $\nu_{sy}CH_2$ stretching absorbance following hydrogenation. (4) The presence of methyl stretching modes and their changes during hydrogenation.

Evidence for methyl and methylene groups was found in the initial and subsequent spectra for the adsorption and reaction of the *n*-butenes. The absorbances at 2965 and 2932 cm^{-1} are assigned to $\nu_{as}CH_3$

and $\nu_{as}CH_2$ vibrations, respectively, based on similar frequency assignments for hydrocarbon groupings in *n*-alkanes (*30, 31*). The 2932-cm^{-1} absorbance ($\nu_{as}CH_2$), in the absence of surface and electronic effects, is normally accompanied by a band of more than half its intensity at 2860 cm^{-1} (*31, 32*), corresponding to $\nu_{sy}CH_2$ (Table 3). Since the band for $\nu_{as}CH_2$ is relatively intense for the initial adsorption of each of the *n*-butenes (Fig. 4), an absorbance for $\nu_{sy}CH_2$ should be observed in the spectra. However, no evidence for an absorbance near 2860 cm^{-1} was observed following the initial adsorption of the *n*-butenes or upon heating these species under vacuum. An absorbance at this frequency was detected following the addition of hydrogen to the surface species.

It is unlikely that the $\nu_{sy}CH_2$ band shifted the 15 cm^{-1} necessary to overlap with the 2875-cm^{-1} band because the $\nu_{as}CH_2$ vibration was shifted at most 5 cm^{-1} from what was expected from a comparison to literature values for typical methylene groups. A more likely cause for the absence of the $\nu_{sy}CH_2$ vibration was that the band was attenuated by the effect of the surface selection rule.

The trimetallabutanes are shown with their methylene hydrogens projecting out of the page. In this configuration the dipole moment for $\nu_{sy}CH_2$, which is in a plane with and bisects the angle formed by H—C—H, is nearly parallel to the metal surface. In contrast, the dipole moment for $\nu_{as}CH_2$ is oriented nearly perpendicular to the surface. While other orientations of the methylene groups are possible for a trimetallabutane, the orientations described above do account for the absence of the $\nu_{sy}CH_2$ stretch.

One type of CH_2 group is proposed to be present and responsible for the absorbance at 2932 cm^{-1}. A terminal C—CH_2—M group was discounted by the 1,1-d_2-butene study (Fig. 7) and the 1-butene study (Fig. 10) which resulted in the same relative $\nu_{as}CH_3$ and $\nu_{as}CH_2$ absorbances. The CH_2 intensity for a terminal group is expected to be attenuated because some of the methylene hydrogens would be substituted by deuterium. The presence of terminal and internal methylene groups C—CH_2—C should lead to absorbances for both types of methylene (*46*), but only one methylene band was observed.

The bands at 2965 and 2932 cm^{-1}, representing $\nu_{as}CH_3$ and $\nu_{as}CH_2$, respectively, shifted down to 2957 and 2925 cm^{-1} upon hydrogenation (compare Figs. 4 and 5). The formation of a new band at approximately 2860 cm^{-1}, corresponding to $\nu_{sy}CH_2$, was also apparent. The bands observed following hydrogenation resembled the absorbances that would be expected for an *n*-alkane in solution (*31, 32*). (The formation of an alkyl-like structure is consistent with early work (*1, 2*).) The shifting may have been caused by a repositioning of the methyl and methylene groups relative to the surface. The appearance of a $\nu_{sy}CH_2$ mode and the alkyl-like methyl and methylene stretching vibrations suggest that the hydrogenated species are more free to move. Hydrogenation of an internal C—M bond as in the 1,1,2- and 1,1,3-trimetallabutanes is consistent with the observed shifts and intensity changes upon hydrogenation.

Following the initial adsorption of the *n*-butenes, a weak band at approximately 2890–2900 cm^{-1} was observed consistently as a shoulder of the intense band at 2880 cm^{-1}. This weak absorbance could be assigned to the νCH vibration of a tertiary carbon atom bound to one or two metal atoms ((—CHM—) or (—CHM_2)), in agreement with similar assignments by other investigators (*3*). The low intensity and frequency of this absorbance correlate well with that of tertiary carbon groupings for *n*-alkanes (Table 3).

The combined observations are consistent with the 1,1,3- and 1,1,2-trimetallabutanes shown in Fig. 13. Di-σ bonding through the α-carbon atom is proposed because this accounts for the apparent absence of terminal methylene groups. Hy-

drocarbon-surface bonding schemes over single crystals and metal films have proposed the presence of di-σ bonding (*47–51*). A third σ-bond to the surface was discounted in our assignments because, assuming nearly sp^3-hybridization of the adsorbed species, this configuration would not allow the C_2 or C_3 carbon atoms to participate in surface bonding.

D. Evidence for Severely Dehydrogenated Species

The results of the hydrogenation studies suggest that other, more severely dehydrogenated C_4 structures coexist on the catalyst surface along with the di- and trimetallabutanes. A significant increase in spectral intensity in the C—H stretching region of the spectrum occurred following the addition of H_2 to the surface species formed from the adsorption of 1-butene onto a hydrogen-covered surface. The partial hydrogenation of the 2,3-, 1,1,2-, and/or 1,1,2-species could not account for this increase. Additionally, *n*-butane was observed in the gas phase following the removal of surface-attached species and this should cause an attenuation of the observed absorbances. The fact that the intensities of the bands in the C—H stretching region increased following the addition of hydrogen to the system suggests that severely dehydrogenated hydrocarbon surface structures were initially present. These findings are in agreement with those of other investigators (*2, 3*) on similar nickel catalysts for the adsorption of 1-butene. A quantitative assessment of the initial concentration of the severely dehydrogenated surface species was not possible. The lack of this information did not influence the outcome of this study since initial spectral contributions from the severely dehydrogenated species were minimal.

The band at 1415 cm^{-1} could be the deformation vibration of a tertiary carbon atom bound to one or two metal atoms ((—CHM—) or (—CHM_2)). This species could result from the dehydrogenation of the initially adsorbed surface species to form a large number of (—CHM—) and (—CHM_2) groups with their C—H bond axes nearly parallel to the surface. In this position, the deformation vibrations for these species would have their dipole moments nearly perpendicular to the metal surface and the resultant band would be appreciably enhanced by the effect of the surface selection rule. No significant absorbance for νC—H would be expected since the dipole moment for this vibration, which is oriented along the C—H axis, would be nearly parallel to the surface.

IV. SUMMARY

The results of this study were used to propose an overall scheme (Fig. 9) for the adsorption and subsequent reaction of *n*-butenes on the Ni/SiO_2 catalyst. The infrared assignments are tentative, pending further work (in progress) on the adsorption of olefins on supported metals. Three classes of surface species are proposed: weakly adsorbed π-allyls and 2,3-dimetallabutanes, strongly adsorbed trimetallabutanes, and severely dehydrogenated C_4 surface structures. In addition, an alkyl-like species was seen following the addition of hydrogen. This alkyl-like structure is represented as a butylidyne in Fig. 9. While infrared evidence supports a sp^3-hybridized carbon species with alkyl-like character, it does not provide insight into the manner by which the terminal carbon is bonded to the surface.

Heating the initially adsorbed species in vacuum resulted in the desorption of the 2,3-dimetallabutane at approximately 40°C to form *n*-butane and the further dehydrogenation and subsequent cracking of the more strongly adsorbed metallabutanes. The C_4 surface structures remained intact at temperatures below 80°C. Higher temperatures resulted in C—C bond scission and the detection of propane in the gas phase.

Allylic species were detected on the catalyst surface during the linear isomerization of the *n*-butenes and are possibly intermedi-

ates in this reaction as well as precursors to the formation of the metallabutanes.

ACKNOWLEDGMENTS

This work was supported by the National Science Foundation under Grant CBT-8319494. The FTIR was funded by the Department of Defense Instrumentation Grant DAAG-29-83-0097.

REFERENCES

1. Pliskin, W. A., and Eischens, R. P., *J. Chem. Phys.* **24,** 482 (1956).
2. Eischens, R. P., and Pliskin, W. A., "Advances in Catalysis," Vol. 10, p. 1. Academic Press, New York, 1958.
3. Morrow, B. A., and Sheppard, N., *Proc. R. Soc. London Ser. A* **311,** 415 (1969).
4. Erkelens, J., and Liefkins, TH. J., *J. Catal.* **8,** 36 (1967).
5. Blyholder, G., Shihabi, D., Wyatt, W. V., and Bartlett, R., *J. Catal.* **43,** 122 (1976).
6. Sheppard, N., and Ward, J. W., *J. Catal.* **15,** 50 (1969).
7. Ravi, A., and Sheppard, N., *J. Phys. Chem.* **76,** 2699 (1972).
8. Busca, G., Zerlia, T., Lorenzelli, V., and Girelli, A., *J. Catal.* **88,** 125 (1984).
9. Eley, D. D., F.R.S., Rochester, C. H., and Scurrell, M. S., *Proc. R. Soc. London Ser. A* **329,** 375 (1972).
10. Avery, N. R., *J. Catal.* **19,** 15 (1970).
11. Chang, C. C., Conner, W. C., Jr., and Kokes, R. J., *J. Amer. Chem. Soc.* **92,** 6709 (1970).
12. Peri, J. B., *J. Phys. Chem.* **69,** 220 (1965).
13. Little, L. H., Sheppard, N., and Yates, D. J. C., *Proc. R. Soc. London Ser. A* **259,** 242 (1960).
14. Beebe, T. P., Jr., Albert, M. R., and Yates, J. T., Jr., *J. Catal.* **96,** 1 (1985).
15. Beebe, T. P., Jr., and Yates, J. T., Jr., *J. Amer. Chem. Soc.* **108,** 663 (1986).
16. Little, L. H., "Infrared Spectra of Adsorbed Species." Academic Press, New York, 1966.
17. Clark, M., Ph.D. thesis, Cambridge University, 1960.
18. Greenler, R. G., Snider, D. R., Witt, D., and Sorbello, R. S., *Surf. Sci.* **118,** 415 (1982).
19. Pearce, H. A., and Sheppard, N., *Surf. Sci.* **59,** 205 (1976).
20. Demuth, J. E., and Ibach, H., *Surf. Sci.* **78,** L238 (1978).
21. Ledoux, M. J., Gault, F. G., Rouchy, A., and Roussy, G., *J. Chem. Soc. Faraday Trans. 1* **76,** 1547 (1980).
22. Huang, K. W., and Ekerdt, J. G., *J. Catal.* **92,** 232 (1985).
23. Dent, A. L., and Kokes, R. J., *J. Phys. Chem.* **73,** 3781 (1969).
24. Dent, A. L., and Kokes, R. J., *J. Amer. Chem. Soc.* **92,** 1092 (1970).
25. Dent, A. L., and Kokes, R. J., *J. Amer. Chem. Soc.* **92,** 6709 (1970).
26. Dent, A. L., and Kokes, R. J., *J. Amer. Chem. Soc.* **92,** 6718 (1970).
27. Prentice, J. D., Lesiunas, A., and Sheppard, N., *J. Chem. Soc. Chem. Commun.*, 76 (1976).
28. Fang, Shui-Min, White, J. M., Campione, T. J., and Ekerdt, J. G., *J. Catal.* **96,** 491 (1985).
29. Campione, T. J., Ph.D. thesis, The University of Texas at Austin, 1985.
30. Bellamy, L. J., "Infrared Spectra of Complex Molecules," 2nd ed., Vol. 2, pp. 1–21. Chapman & Hall, London, 1980.
31. Wexler, A. S., *Appl. Spectrosc. Rev.* **1,** 29 (1967).
32. Jones, R. N., *Spectrochim. Acta* **9,** 235 (1957).
33. Somorjai, G. A., "Chemistry in Two Dimensions: Surfaces," p. 196. Cornell Univ. Press, Ithaca, N.Y., 1981.
34. Heimbach, P., and Traunmuller, R., *Ann. Chem.* **727,** 208 (1969).
35. Manojlovic-Muir, L., Muir, J. W., and Ibers, J. A., *Discuss. Faraday Soc.* **47,** 84 (1969).
36. Fritz, H. P., Schwarzhans, K. E., and Sellman, D., *J. Organomet. Chem.* **6,** 551 (1966).
37. Quinn, H. W., McIntyre, J. S., and Peterson, D. J., *Canad. J. Chem.* **40,** 1103 (1962).
38. Lukehart, C. M., "Fundamental Transition Metal Organometallic Chemistry," p. 167. Brooks/Cole Pub. Co., Monterey, Calif., 1985.
39. Mason, R., and Russell, D. R., *Chem. Commun.* No. 1, 26 (1966).
40. Fischer, E. O., and Burger, G., *Chem. Ber.* **94,** 2409 (1961).
41. Fischer, E. O., and Burger, G., *Z. Naturforsch. B: Anorg. Chem., Org. Chem.* **16,** 77 (1961).
42. Dent, A. L., and Kokes, R. J., *J. Phys. Chem.* **75,** 487 (1971).
43. Murdoch, von H. D., and Weiss, E., *Helv. Chim. Acta* **45,** 1927 (1962).
44. Faller, J. W., and Davison, A., *Inorg. Chem.* **6,** 179 (1967).
45. McClellan, W. R., Hoehn, H. H., Cripps, H. N., Muetterties, E. L., and Howk, B. W., *J. Amer. Chem. Soc.* **83,** 1601 (1961).
46. Gussoni, M., Abbate, S., and Sanvito, R., *J. Mol. Struct.* **75,** 177 (1981).
47. Koestner, R. J., Frost, J. C., Stair, P. C., Van Hove, M. A., and Somorjai, G. A., *Surf. Sci.* **116,** 85 (1982).
48. Baro, A. M., and Ibach, H., *J. Chem. Phys.* **74,** 4194 (1981).
49. Kesmodel, L. L., Dubois, L. H., and Somorjai, G. A., *J. Chem. Phys.* **70,** 2180 (1979).
50. Ibach, H., and Mills, D. L., "Electron Spectroscopy for Surface Analysis," p. 326. Academic Press, New York, 1982.
51. Albert, M. R., Sneddon, L. G., Plummer, E. W., and Gustafsson, T., *Surf. Sci.* **117,** 491 (1982).